

Contact angles in the presence of an electrical field

A L Kupershtokh

National Research Novosibirsk State University, 1 Pirogova str., Novosibirsk, 630090, Russia

E-mail: skn@hydro.nsc.ru

Abstract. Three-dimensional computer simulations of the dynamics of sessile droplets in an electric field and without it are carried out on the basis of the lattice Boltzmann method (LBM). The dielectric droplets are placed on the surface of the lower electrode. The electrical and hydrodynamic parts of the problem are solved simultaneously. After application of an electric field, the droplets begin to lengthen in the field direction. The contact angle is measured after the droplet acquires its equilibrium shape. It is shown that the contact angle slightly increases with increasing the electric field due to electrostatic forces. Above a certain critical value of the electrical Bond number, the droplets cannot acquire a stable form, the elongation becomes unlimited, and the droplets are destroyed.

1. Introduction

Earlier in [1], it was shown that for some liquid dielectrics (ethanol, hexanol, heptanol, octanol, etc.), the contact angle of a droplet lying on a solid surface in a gravitational field slightly increases with increasing electric field E . The question is discussed about the fact that the surface tension of the liquid also changes. Similar results were obtained in [2] where nanodroplets were simulated by the molecular dynamics method. At the same time, for a number of other liquid dielectrics, experiments show a decrease in the contact angle under the action of electric fields.

In this paper, these processes were simulated for the first time in numerical experiments in the framework of a continuous medium.

To simulate droplets placed on the electrode surface, it is necessary not only to calculate the distribution of electric fields, but also to determine the shape of droplets after the application of an electric field. A three-dimensional electrohydrodynamic model of the dynamics of sessile droplets is developed that takes into account a surface tension and the processes of evaporation and condensation at the vapor-liquid interfaces. In these simulations, the lattice Boltzmann method (LBM) is used. At this stage of researches, the calculations are carried out for dielectric fluids.

2. Lattice Boltzmann method for hydrodynamic part of simulations

To describe the fluid flow with liquid-vapor interfaces, the method of lattice Boltzmann equations with interactions between nodes (pseudopotential method) was used [3-5]. The method is essentially a method of characteristics for the Boltzmann equation with a discrete set of velocities $\{\mathbf{c}_k\}$. The calculations were carried out on a three-dimensional cubic lattice with 19 pseudoparticle velocity vectors \mathbf{c}_k (D3Q19).

The fluid states are described by the set of distribution functions $N_k(\mathbf{x}, t)$ (pseudoparticles) in every node. At every time step, the values of $N_k(\mathbf{x}, t)$ are transferred along the characteristics to the



18 neighbor nodes. After that, these values are redistributed in velocity space in every node by the collision operator $\Omega_k = (N_k^{eq}(\rho, \mathbf{u}) - N_k(\mathbf{x}, t)) / \tau$. Hence, we have the equation

$$N_k(\mathbf{x} + \mathbf{c}_k \Delta t, t + \Delta t) = N_k(\mathbf{x}, t) + \Omega_k(\{N_k(\mathbf{x}, t)\}) + \Delta N_k. \quad (1)$$

Here, ΔN_k is the change of the distribution functions because of the action of body forces (internal and external). Hydrodynamic variables, such as the fluid density ρ and velocity \mathbf{u} , can be calculated as

$$\rho = \sum_{k=0}^b N_k \quad \text{and} \quad \rho \mathbf{u} = \sum_{k=1}^b \mathbf{c}_k N_k. \quad (2)$$

To simulate the liquid-vapor phase transitions, internal forces between the neighbor nodes were introduced. The total force acting on a node is expressed as the gradient of the pseudopotential $U = P(\rho, T) - \rho\theta$ [3]. The isotropic hybrid finite-difference approximation for the gradient operator proposed in [4] is used. We use the Exact Difference Method (EDM) [5,6] to implement the body force term in LBM. The van der Waals equation of state written in the dimensionless variables is used for fluid. For the hydrodynamic problem, no-slip boundary conditions are fulfilled on the electrodes. In x and y directions, the periodic boundary conditions are used.

For three-dimensional simulations, we use two multi-processor graphics cards (GPUs) Titan-Xp and Titan-V (3840 and 5120 cores, respectively). The total amount of fast memory is 24 GB. CUDA technology is used for parallel calculations on all cores of GPUs.

The values of the contact angle depend on the forces of interaction of fluid with the solid surface. For this purpose, the forces acting on the fluid node \mathbf{x} adjacent to a solid surface from the side of five neighboring nodes of the solid are introduced into the LBM method (figure 1). The total force can be written as

$$\mathbf{F}(\mathbf{x}) = B\Phi(\mathbf{x}) \sum_{i=1}^5 w(\mathbf{e}_i) \Phi_{\text{solid}}(\mathbf{x} + \mathbf{e}_i) \cdot \mathbf{e}_i. \quad (3)$$

Here, the function for fluid is equal to $\Phi(\mathbf{x}) = \sqrt{\rho\theta - P(\rho, T)}$ [4]. The values of Φ_{solid} at nodes of solid surface take the same values as at the nearest nodes of fluid $\Phi_{\text{solid}}(\mathbf{x} + \mathbf{e}_5) = \Phi(\mathbf{x})$ [4] (figure 1). The wettability of the solid surface is determined by the parameter B (adhesion parameter). A contact angle of 90° is obtained with the parameter $B = 1$.

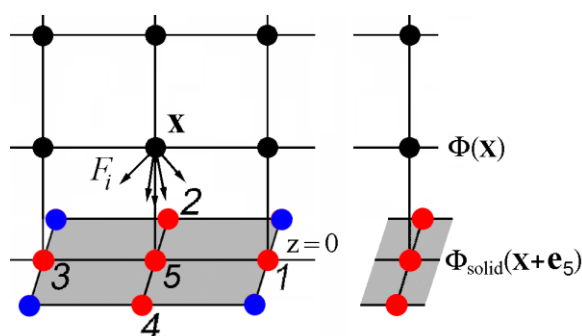


Figure 1. Forces acting on a fluid node \mathbf{x} due to the interaction with the nearest five nodes of the solid surface.

3. Electric field calculations and electrostatic body forces

To take into account electrostatic forces acting in the volume of non-uniform dielectric we use the Helmholtz equation [7]

$$\mathbf{F} = -\frac{\varepsilon_0 E^2}{2} \nabla \varepsilon + \frac{\varepsilon_0}{2} \nabla \left[E^2 \rho \left(\frac{\partial \varepsilon}{\partial \rho} \right)_T \right], \quad (4)$$

where, ε_0 is the dielectric constant for vacuum, ε is the dielectric permittivity of fluid, E is the magnitude of an electric field and ρ is the density of fluid.

To take into account the effect of electrical body forces, it is necessary to determine the distribution of the electric field in an inhomogeneous dielectric. The calculation of the electric field potential $\varphi(\mathbf{x}, t)$ between flat parallel electrodes placed at the distance d is performed at each time step. For this purpose, we use the well-known method of simple iterations. The values for the electric field potential $\varphi=0$ at the lower electrode and $\varphi=V$ at the upper electrode are set as the boundary conditions. In the x and y directions, the potential of electric field is taken as a periodic function. The variations in the dielectric constant $\varepsilon(\mathbf{x}, t)$ of the dielectric fluid in space and time are taken into account. We use the well-known Clausius–Mossotti formula for the dielectric constant of a non-polar fluid

$$\varepsilon = 1 + \frac{3\alpha\rho}{1 - \alpha\rho}, \quad (5)$$

where α is the polarizability. After that, the electric field can be calculated as $\mathbf{E}(\mathbf{x}, t) = -\nabla\varphi(\mathbf{x}, t)$. The electrical and hydrodynamic parts of the problem are solved simultaneously.

4. Simulation results

Three-dimensional simulations of the dynamics of sessile droplets are carried out on the basis of LBM. The surface tension and processes of evaporation and condensation are taken into account at the liquid-vapor interfaces. The droplet of given volume V is placed on the surface of the lower electrode in gravity field. The initial shape of the droplet is a segment of ball. In numerical experiments, a fluid was selected that is close to hexanol in the most important parameters. The dielectric constant for hexanol $\varepsilon=13.3$. The ratio of gravity to surface tension forces is determined by the Bond number $Bo = \rho g R_0^2 / \sigma$, which corresponds approximately to 2 for all simulations. Here, ρ is the density of the liquid, R_0 is the characteristic radius of a droplet and σ is the surface tension. After DC voltage applied, the droplet tends to lengthen in the direction of the electric field. If the voltage is less than a certain critical value, the droplet acquires its equilibrium shape (figures 2 and 3) after the initial oscillations decay in time ($\sim 0.3 \cdot 10^6 - 3 \cdot 10^6$ steps). In another case, the elongation becomes unstable.

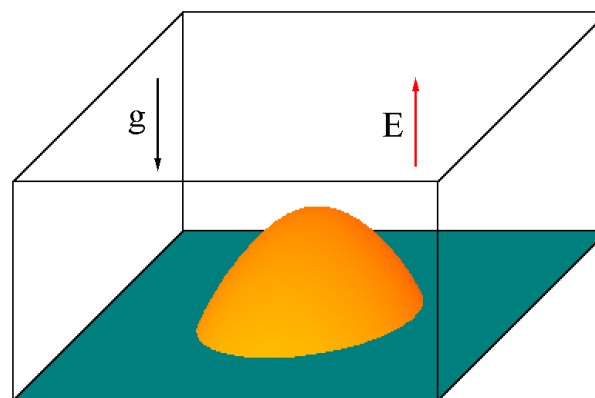


Figure 2. Quasistationary shape of droplet after ≈ 2 million time steps. $B = 1.0417$, $\varepsilon = 13.3$, $Bo = 2$. The electric Bond number is equal to 15.2. $t = 1.9 \cdot 10^6$. Lattice $432 \times 432 \times 224$.

The dimensionless parameter governing the droplet behavior in the electric field is the electrical Bond number

$$Bo_E = \frac{\epsilon_0 E^2}{2} (\epsilon_l - 1) \frac{R_0}{2\sigma} \tag{6}$$

Here, ϵ_l is the dielectric permittivity of the liquid phase, $E = V/d$ is the mean value of the electric field in the gap. The value of $Bo_E = 8.5$ corresponds to $E \sim 40$ kV/cm for $R_0 = 5$ mm and $\sigma \approx 0.03$ N/m in physical units.

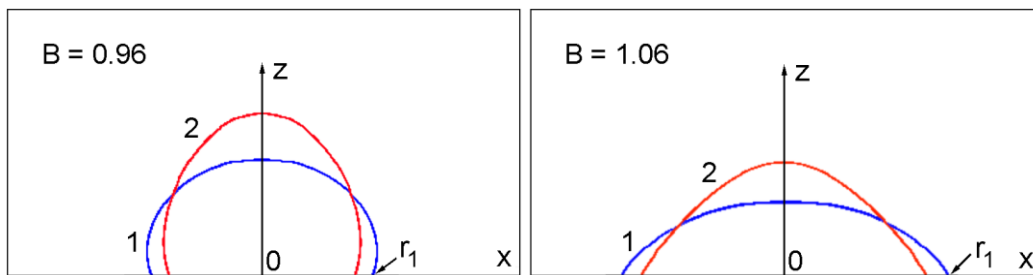


Figure 3. Stationary droplet profiles (central $x - z$ cross sections) before (curves 1) and after application of electric field (curves 2). The values of parameter B are 0.96 and 1.06.

The method of determination of contact angle of an axisymmetric sessile droplet in a gravitational field was proposed in the work [8]. The authors used the profile of droplet shape for analysis. This method can be used for droplets only in a uniform field of forces. Unfortunately, this method cannot be applied to a droplet in an electric field, because the electric field becomes not uniform if a dielectric droplet is present.

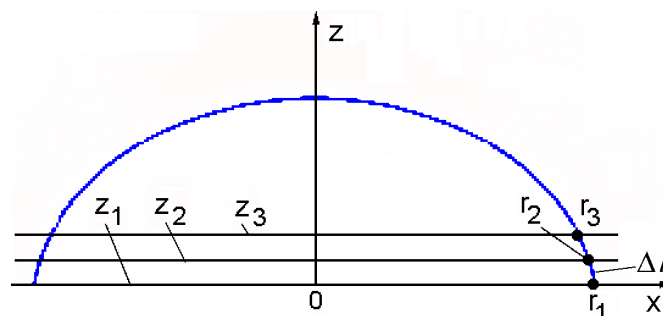


Figure 4. Typical profile of an axisymmetric droplet shape (central $x - z$ cross section).

The radius of curvature R_c of the droplet directly near the substrate is calculated using an inscribed circle that passes through three points on the droplet profile (figure 4) with coordinates $(r_1, z_1), (r_2, z_2)$, and (r_3, z_3) . Here $z_1 = 1, z_2 = 10$, and $z_3 = 20$ are the z coordinates of horizontal planes parallel to substrate. The values of radii r_1, r_2 , and r_3 are averaged over the nodes (more than 1000) that belong to entire profile circle on each plane z_1, z_2 and z_3 .

The first method to derive the value of contact angle is to use directly this circle approximation

$$\theta_R = \pi/2 + \arctan(z_0/(r_1 - x_0)), \tag{7}$$

where x_0 and z_0 are the coordinates of the center of the approximating circle.

The second method is the well-known tangent method

$$\theta_t = \pi/2 - \arctan(\Delta r/\Delta z) + \Delta l/(2R_c), \tag{8}$$

where $\Delta r = r_2 - r_1$ and $\Delta z = z_2 - z_1$ are the differences of r and z coordinates between two reference points, $\Delta l \approx \sqrt{\Delta r^2 + \Delta z^2}$ is the approximate arc length of the inscribed circle between points 1 and 2 (figure 4). The first two terms are the angle calculated using the chord, and the last term is the correction, which takes into account the angle between the chord and the corresponding small arc Δl .

Both these methods give the values that very close one to another. These methods are tested for the case of a contact angle without an electric field. The dependence of contact angle on parameter wettability B is shown in figure 5.

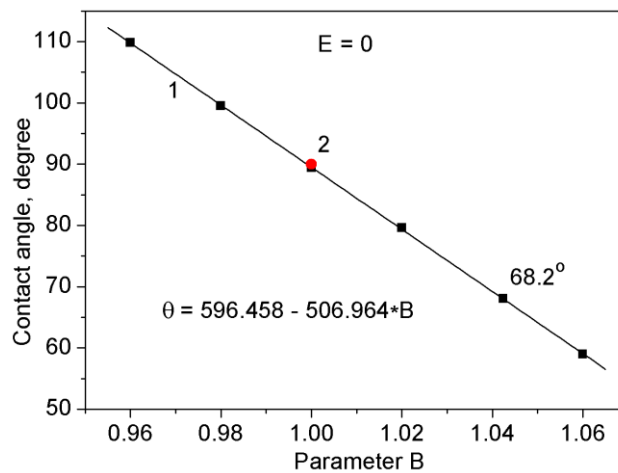


Figure 5. The values of contact angle (curve 1) obtained in simulations (■) without electric field vs. parametr B (adhesion level). Point 2(●) is related to the theoretical value of 90° at $B = 1.00$.

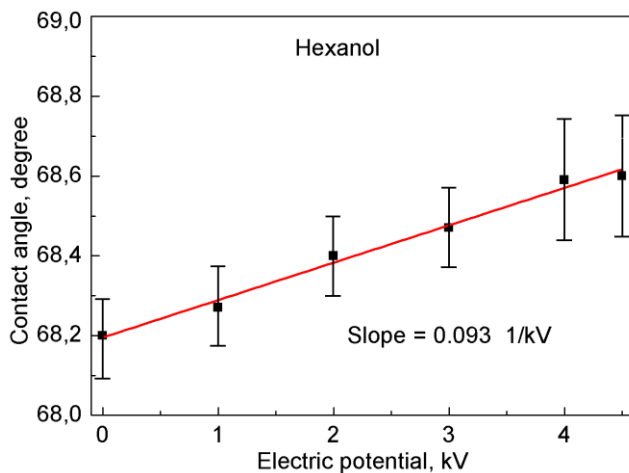


Figure 6. The dependence of the experimental values of the contact angle on the applied voltage for a droplet of hexanol [1]. Each point was averaged over nine runs.

Experimental data on contact angles in an electric field for some liquid dielectrics (ethanol, hexanol, heptanol, octanol, etc.) are presented in [1]. Figure 6 shows the dependence of the contact angle on the applied voltage for hexanol ($\text{CH}_3(\text{CH}_2)_5\text{OH}$). Since the experimental values had some scatter (from 0.25° to 0.4°) [1], each point was averaged over nine experiments. The dependence of the experimental data on hexanol [1] on the electric Bond number Bo_E (figure 7, line 1) is more informative. Here, our data obtained by numerical simulation are also shown. The calculated data also have a scatter from 0.3° to 0.6° at varying droplet volume due to the discreteness of the computational

grid. The linear approximation of the simulation results (figure 7, line 2) is slightly higher than the experimental data for hexanol (line 1), since the parameter $B = 1.0417$ is chosen slightly less than necessary in accordance with the line on figure 5 ($\theta_0 = 68.2^\circ$ at $B = 1.0424$).

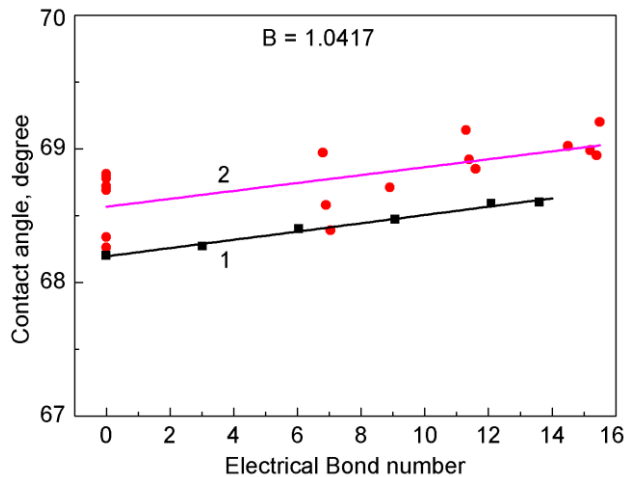


Figure 7. The dependence of contact angle on electric Bond number.

1(■) – experimental data [1] for hexanol.
2(●) – our numerical experiments and linear approximation.

Conclusions

Three-dimensional simulations of the dynamics of sessile droplets in an electric field and without it are carried out on the basis of LBM. The dielectric droplets located on the surface of the lower electrode begin to elongate under the action of the electric field. After the droplet acquires its equilibrium shape, the contact angle is measured. It is shown that the contact angle slightly increases with increasing the electric field due to electrostatic forces. This result is in reasonable agreement with the experimental data [1]. If the electric Bond number becomes greater than a certain critical value, the elongation becomes unlimited, and droplets are destroyed.

Acknowledgements

The study was supported by the Russian Science Foundation: grants Nos. 16-19-10229 (the method for determining contact angles of sessile droplets in an electric field) and 18-19-00538 (three-dimensional simulations of droplets under the action of an electric field).

References

- [1] Bateni A, Laughton S, Tavana H, Susnar S S, Amirfazli A and Neumann A W 2005 *J. Colloid Interface Sci.* **283** 215–22
- [2] Song F, Ma L, Fan J, Chen Q, Zhang L and Li B Q 2018 *Nanomaterials* **8**(5) 340–51
- [3] Qian Y H and Chen S 1997 *Int. J. Mod. Phys. C* **8**(4) 763–71
- [4] Kupershtokh A L, Medvedev D A and Karpov D I 2009 *Computers and Mathematics with Applications* **58**(5) 965–74
- [5] Kupershtokh A L 2010 *Computers and Mathematics with Applications* **59**(7) 2236–45
- [6] Kupershtokh A L 2004 *Proc. 5th International EHD Workshop (Poitiers) (Poitiers: Universite de Poitier, France)* p 241–6
- [7] Landau L D and Lifshitz E M 1959 *Electrodynamics of Continuous Media* (Oxford: Pergamon Press)
- [8] Marchuk I V, Cheverda V V, Strizhak P A and Kabov O A 2015 *Thermophysics and Aeromechanics* **22**(3) 297–303